

(except those to hydrogen) within the molecule.

NMR Simulations and Analyses. The $^{19}\text{F}\{^1\text{H}\}$ spectrum of $\text{P}(\text{C}_6\text{F}_5)_2\text{Ph}_2$ was analyzed by iterative least-squares fitting using the program UEA/NMR 11²³ running on a SUN-4/260. The best fit to the spectrum of **3** was then obtained by manual adjustment of the appropriate parameters, and direct comparison between the simulated and experimental spectra. Dynamic NMR spectra were simulated using the DNMR3 program,²⁴ modified to permit calculation of spectra as a sum of several independent exchanging systems.

Preparation of $[(\eta^5\text{-C}_5\text{H}_5)\text{Fe}(\text{CO})\{\text{P}(3,5\text{-C}_6\text{H}_3\text{F}_2)_3\}\text{COMe}]$ (2**).** A deoxygenated solution of $[(\eta^5\text{-C}_5\text{H}_5)\text{Fe}(\text{CO})_2\text{Me}]$ (0.69 g, 3.6 mmol) and $\text{P}(3,5\text{-C}_6\text{H}_3\text{F}_2)_3$ (1.3 g, 3.6 mmol) in tetrahydrofuran/cyclohexane (2:1) was photolyzed with a Hanovia 125-W medium-pressure Hg arc lamp for 5.5 h. Volatiles were removed from the resulting red solution under vacuum to yield a red oil which was shown by ^1H NMR to be an 8:3 mixture of $[(\eta^5\text{-C}_5\text{H}_5)\text{Fe}(\text{CO})\{\text{P}(3,5\text{-C}_6\text{H}_3\text{F}_2)_3\}\text{Me}]$ and $[(\eta^5\text{-C}_5\text{H}_5)\text{Fe}(\text{CO})_2\text{Me}]$ (the methyl resonance for the phosphinated derivative showing characteristic coupling to phosphorus $J_{\text{P-H}} = 8$ Hz). The oil was taken up in 35 mL of THF and after addition of 1 equiv of $\text{BF}_3\cdot\text{Et}_2\text{O}$ (43 μL , 3.6 mmol) charged to a Fisher-Porter bottle and pressurized with CO

(120 psi) for 3 days. The vessel was then depressurized and of 50 mL/ H_2O added. The mixture was extracted with dichloromethane (3×50 mL) and dried over Na_2SO_4 ; volatiles were removed under vacuum to give a red brown oil. Chromatography on Grade I alumina with CH_2Cl_2 -hexane allowed facile separation of the less polar starting material and methyl intermediate $[(\eta^5\text{-C}_5\text{H}_5)\text{Fe}(\text{CO})\{\text{P}(3,5\text{-C}_6\text{H}_3\text{F}_2)_3\}\text{Me}]$ from the carbonyl inserted product. Collection of the final orange band and removal of solvent under vacuum gave analytically pure **2** (0.41 g, 0.72 mmol, 20%) as a bright orange foam. The collected starting material and phosphine exchanged methyl intermediate could be effectively recycled through the procedure. Anal. Calcd for $\text{C}_{26}\text{H}_{17}\text{F}_6\text{Fe}_1\text{O}_2\text{P}_1$: C, 55.55; H, 3.05. Found: C, 55.70; H, 4.23. IR (CH_2Cl_2): ν_{max} 1928 (CO), 1608 ($\text{C}=\text{O}$) cm^{-1} . ^1H NMR (CDCl_3): δ 6.85-7.1 (9 H, m, $\text{C}_6\text{H}_3\text{F}_2$), 4.49 (5 H, d, $J = 1.3$ Hz, C_5H_5), 2.47 (3 H, s, CH_3). $^{13}\text{C}\{^1\text{H}\}$ (CDCl_3): δ 272.51 (d, $J_{\text{P-C}} = 22.5$ Hz, $\text{C}=\text{O}$), 219.27 (d, $J_{\text{P-C}} = 30.0$ Hz, $\text{C}=\text{O}$), 162.73 (d of d of d, $J_{\text{C-F}} = 253.7$ Hz, $J_{\text{C-P}} = 16.5$ (11.8) Hz, $J_{\text{C-P}} = 11.8$ (16.5) Hz, C_{meta}), 139.64 (d of t, $J_{\text{C-P}} = 40.8$ Hz, $J_{\text{C-F}} = 6.7$ Hz, C_{ipso}), 116.00 (d of d, $J_{\text{C-F}} = 26.1$ Hz, $J_{\text{C-P}} = 11.3$ Hz, C_{ortho}), 106.41 (t, $J_{\text{C-F}} = 25.3$ Hz, C_{para}), 85.26 (s, C_5H_5), 52.03 (s, CH_3). $^{19}\text{F}\{^1\text{H}\}$ (CDCl_3): δ -109.53 (d, $J_{\text{P-F}} = 4.6$ Hz). Mass spectral analysis: $m/z = 562$.

(23) Loomes, D. J.; Harris, R. K.; Anstey, P. *The NMR Program Library*; SERC Daresbury Laboratory: Warrington, UK.

(24) Stephenson, D. S.; Binsch, G. *J. Magn. Reson.* 1978, 32, 141.

Acknowledgment. We thank BP International Ltd. for a Venture Research Award.

Cupric Ion Location and Adsorbate Interactions in Cupric Ion Exchanged H-SAPO-5 Molecular Sieve As Determined by Electron Spin Resonance and Electron Spin Echo Modulation Spectroscopies

Xinhua Chen and Larry Kevan*

Contribution from the Department of Chemistry, University of Houston, Houston, Texas 77204-5641. Received September 24, 1990

Abstract: Locations of Cu^{2+} ions exchanged into H-SAPO-5 and interactions of Cu^{2+} ions with water, ammonia, and methanol have been investigated by electron spin resonance and electron spin echo modulation techniques. It has been determined that Cu^{2+} ions locate at a position inside a 12-ring channel, close to the center of a 6-ring window in hydrated, ammonia-adsorbed, and methanol-adsorbed CuH-SAPO-5 samples. The Cu^{2+} ion directly coordinates to three framework oxygens in all systems studied; it also directly coordinates to three water molecules in the hydrated sample and to three ammonia molecules in the ammonia-adsorbed sample. In methanol-adsorbed samples, the Cu^{2+} ion directly coordinates to two methanol molecules and indirectly coordinates to one methanol molecule at a greater distance. The more bulky size of methanol molecules compared to water and ammonia is likely the cause of fewer methanol molecules directly coordinated to Cu^{2+} .

Introduction

Silicoaluminophosphate (SAPO) molecular sieves form a new class of microporous crystalline materials comparable to the well-known zeolites, or aluminosilicate molecular sieves. Zeolites, which have been widely used for adsorption and catalysis, have pores or channels formed by aluminum and silicon tetrahedra linked by oxygen bridges. Substitution of other elements for Al and/or Si in the molecular sieve framework can yield various kinds of new materials. In 1982, Wilson et al. reported the synthesis of aluminophosphate (AlPO_4) molecular sieves.^{1,2} The structures of AlPO_4 molecular sieves include novel structure types, such as $\text{AlPO}_4\text{-5}$, as well as structure types analogous to certain zeolites, such as $\text{AlPO}_4\text{-37}$ (faujasite structure). In 1984, Lok et al. reported the synthesis of SAPO molecular sieves,^{3,4} which can be

viewed as silicon-substituted AlPO_4 . The numbering of structure types of SAPO follows that of AlPO_4 , so that SAPO-5 denotes the SAPO molecular sieve that possesses the same framework structure as $\text{AlPO}_4\text{-5}$.

The SAPO-5 molecular sieve is composed of 4-ring, 6-ring, and 12-ring straight channels, which are interconnected by 6-ring windows (Figure 1). Because the SiO_2 tetrahedron is electrically neutral and, in SAPO-5, the number of AlO_2^- tetrahedra is slightly greater than the PO_2^+ tetrahedra, the SAPO-5 framework is slightly negatively charged.⁵ The framework negative charges are balanced by H^+ ions and the cationic form of the templating agent in the as-synthesized SAPO-5 and by H^+ ions only in H-SAPO-5, the calcined form of SAPO-5. H^+ ions in H-SAPO-5

(1) Wilson, S. T.; Lok, B. M.; Flanigen, E. M. U.S. Patent 4 310 440, 1982.

(2) Wilson, T. T.; Lok, B. M.; Messina, C. A.; Cannan, T. R.; Flanigen, E. M. *J. Am. Chem. Soc.* 1982, 104, 1146-1147.

(3) Lok, B. M.; Messina, C. A.; Patton, R. L.; Gajek, R. T.; Cannan, T. R.; Flanigen, E. M. U.S. Patent 4 440 871, 1984.

(4) Lok, B. M.; Messina, C. A.; Patton, R. L.; Gajek, R. T.; Cannan, T. R.; Flanigen, E. M. *J. Am. Chem. Soc.* 1984, 106, 6092-6093.

(5) Flanigen, E. M.; Lok, B. M.; Patton, R. L.; Wilson, S. T. In *New Developments in Zeolite Science and Technology*; Murakami, Y., Iijima, A., Ward, J. W., Eds.; Proceedings of the 7th International Zeolite Conference; Elsevier: Amsterdam, 1986; pp 103-112.

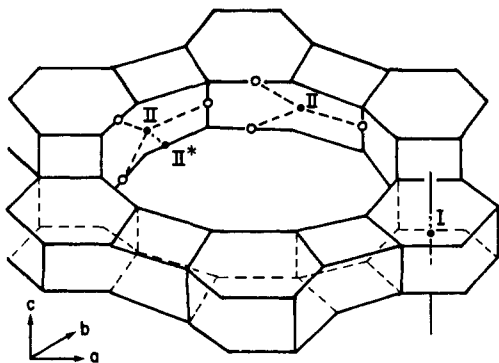


Figure 1. SAPO-5 structure. Cation sites are proposed by analogy with zeolite X.

can be exchanged to some extent by Cu^{2+} ions and the exchanged product is denoted CuH-SAPO-5.

Electron spin resonance (ESR) and electron spin echo modulation (ESEM) spectroscopies have been used quite effectively for probing Cu^{2+} ions exchanged into zeolites.⁶⁻¹³ Parameters obtained from ESR can be used to deduce the local symmetry of the transition-metal ions, and analysis of ESEM signals yields the number of surrounding adsorbate nuclei and their interaction distances and weak isotropic hyperfine coupling constants.¹⁴ Combining both ESR and ESEM techniques provides valuable data for deciphering the locations of the transition-metal ions exchanged into molecular sieves and the metal ion-adsorbate interactions.

The present ESR/ESEM study is the first to investigate the location and adsorbate interactions of Cu^{2+} ions exchanged into SAPO molecular sieves. The location of Cu^{2+} in CuH-SAPO-5 has been determined to be close to the center of a 6-ring window on one side of a 12-ring channel, coordinating to three framework oxygens and three adsorbate molecules in hydrated and ammonia-adsorbed CuH-SAPO-5. It has also been determined that a Cu^{2+} ion at the same location directly coordinates to only two methanol molecules but indirectly coordinates to one additional methanol molecule at a greater distance. These new structural results are relevant to Cu^{2+} -catalyzed reactions in SAPO molecular sieves.

Experimental Section

SAPO-5 molecular sieve was synthesized according to a Union Carbide patent (example 13)³ with modifications suggested by Professor M. Davis of Virginia Polytechnic University. H_3PO_4 (85%, Fisher Chemical), $\text{Al}_2\text{O}_3 \cdot 2\text{H}_2\text{O}$ (Vista Chemical), tripropylamine (Aldrich Chemical), fumed silica (Sigma Chemical), and deionized water were used to produce a gel with the following molar composition:



The gel was sealed in a Teflon-lined stainless steel pressure vessel and heated at 150 °C for 45 h at autogenous pressure. The reaction system was quenched and the product was washed three times before filtering. The X-ray diffraction patterns of the synthesized material agree with that of SAPO-5 in the literature.^{3,5} The organic templating agent, tripropylamine, was removed by heating the as-synthesized SAPO-5 at 400 °C in the presence of O_2 flow for 72 h. Cu^{2+} was exchanged into H-SAPO-5 by mixing 1 g of H-SAPO-5, 15 mL of 1×10^{-3} M $\text{Cu}(\text{NO}_3)_2$

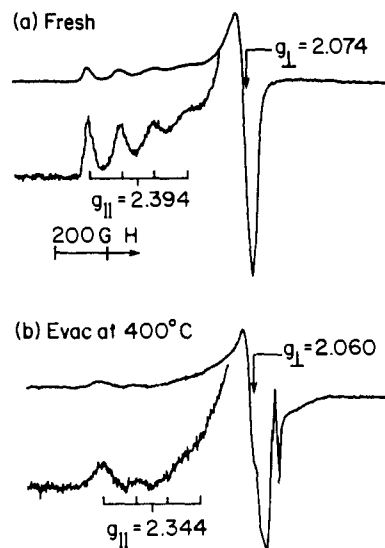


Figure 2. ESR spectra recorded at 77 K for CuH-SAPO-5: (a) fresh; (b) evacuated at 400 °C.

solution, and 85 mL of deionized water and stirring at ca. 70 °C for 8 h. The exchanged sample was filtered and then washed with hot water three times in order to remove excess Cu^{2+} ions from the outer surface of the sample. The air-dried sample is termed "fresh" hereafter. Other samples were prepared by dehydrating the fresh sample at various temperatures under vacuum for ca. 18 h to a residual pressure of 1×10^{-4} Torr. Samples evacuated at temperatures higher than 150 °C were exposed to 760 Torr of oxygen at the evacuation temperatures to reoxidize reduced copper ions to Cu^{2+} , followed by evacuation at room temperature to remove oxygen. Samples dehydrated at 400 °C in this way are called activated. The activated samples were exposed to adsorbates at their room temperature vapor pressure for 18 h prior to ESR and ESEM measurements. The adsorbates used were D_2O (Aldrich Chemical), $^{15}\text{NH}_3$ (ICN Life Sciences group), CH_3OD , and CD_3OH (Stohler Isotope Chemicals). On the basis of the internal consistency of similar studies in X-zeolites,¹¹ it is unlikely that any significant exchange between residual hydroxyl centers on the zeolite and the deuterated adsorbates occurs at room temperature. But even if some such exchange occurs the results are unchanged within the accuracy of the experiment since the deuterated adsorbate is in great excess.

ESR spectra were recorded at 77 K on a modified Varian E-4 ESR spectrometer, which is interfaced to a Tracor Northern TN-1710 signal averager. Each spectrum was obtained by multiple scans to achieve a satisfactory signal-to-noise ratio. Each acquired spectrum with 1024 data points was transferred from the signal averager to an IBM PC/XT compatible computer for storage, analysis, and plotting. The magnetic field was calibrated with a Varian E-500 gaussmeter. The microwave frequency was monitored by a Hewlett-Packard HP5342A microwave frequency counter.

ESEM signals were recorded at 4 K on a home-built ESE spectrometer.¹⁶ Both two-pulse and three-pulse ESE experiments were carried out. In a two-pulse experiment, pulse widths of 40–80 ns were used to generate the pulse sequence of $90^\circ-\tau-180^\circ$. In a three-pulse experiment, pulse widths of 40–40–40 ns were used to generate the pulse sequence of $90^\circ-\tau-90^\circ-T-90^\circ$, τ being fixed at 0.28 μs in order to suppress ^{27}Al modulation. Two-pulse glitches in a three-pulse ESEM spectra were eliminated by using the phase cycling sequence of $[(000) + (\pi\pi 0)] - [(\pi\pi\pi) + [(00\pi)]]$.¹⁷ The collected ESEM data were transferred to an HCP386 IBM PC compatible computer for analysis. ESEM simulations were based on the method given by Dikanov et al.¹⁸ Simulated ESEM patterns were calculated on a VAX mainframe computer and then downloaded to the HCP386 computer for graphical comparison with the experimental data.

Results

ESR spectra of fully hydrated (fresh) and fully dehydrated (activated) samples (Figure 2) show that the Cu^{2+} ions have an

(6) Narayana, M.; Kevan, L. *J. Chem. Phys.* **1983**, *78*, 3573–3578.

(7) Ichikawa, T.; Kevan, L. *J. Am. Chem. Soc.* **1983**, *105*, 402–406.

(8) Narayana, M.; Kevan, L. *J. Phys. Chem.* **1983**, *16*, 361–367.

(9) Ichikawa, T.; Kevan, L. *J. Am. Chem. Soc.* **1982**, *104*, 1481–1483.

(10) Anderson, M. W.; Kevan, L. *J. Phys. Chem.* **1987**, *91*, 2926–2930.

(11) Kevan, L. *Rev. Chem. Intermed.* **1987**, *8*, 53–85.

(12) Anderson, M. W.; Kevan, L. *J. Phys. Chem.* **1986**, *90*, 3206–3212.

(13) Sass, C. E.; Kevan, L. *J. Phys. Chem.* **1989**, *93*, 4669–4674.

(14) Kevan, L. In *Time Domain Electron Spin Resonance*; Kevan, L., Schwartz, R. N., Eds.; John Wiley: New York, 1979; Chapter 8.

(15) Wilson, S. T.; Lok, B. M.; Messina, C. A.; Cannan, T. R.; Flanigen, E. M. In *Intrazeolite Chemistry*; Stucky, G. D., Dwyer, F. G., Eds.; ACS Symposium Series 218, American Chemical Society: Washington, DC, 1983; pp 79–106.

(16) Narayana, P. A.; Kevan, L. *Magn. Reson. Rev.* **1983**, *7*, 239–274.

(17) Fauth, J. M.; Schweiger, A.; Brauschweiler, L.; Forrer, J.; Ernst, R. R. *J. Magn. Reson.* **1986**, *66*, 74.

(18) Dikanov, S. A.; Shubin, A. A.; Parmon, V. N. *J. Magn. Reson.* **1981**, *42*, 474–487.

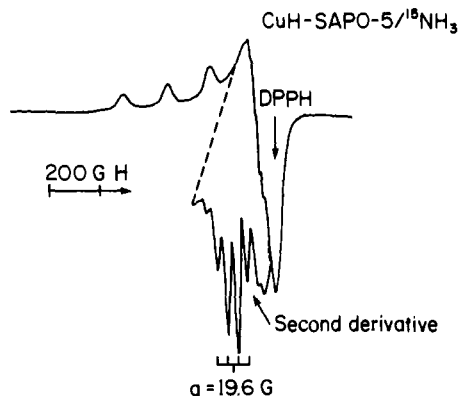


Figure 3. ESR spectrum at 77 K of CuH-SAPO-5 with adsorbed $^{15}\text{NH}_3$.

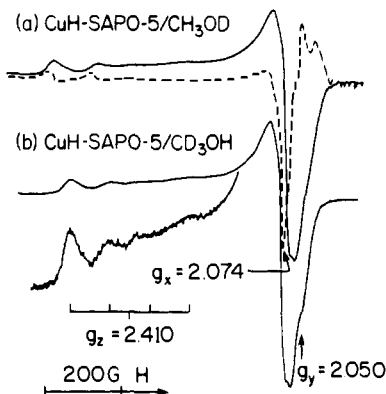


Figure 4. ESR spectra at 77 K of CuH-SAPO-5 with adsorbed (a) CH_3OD and (b) CD_3OH . Dashed lines represent the second-derivative spectrum.

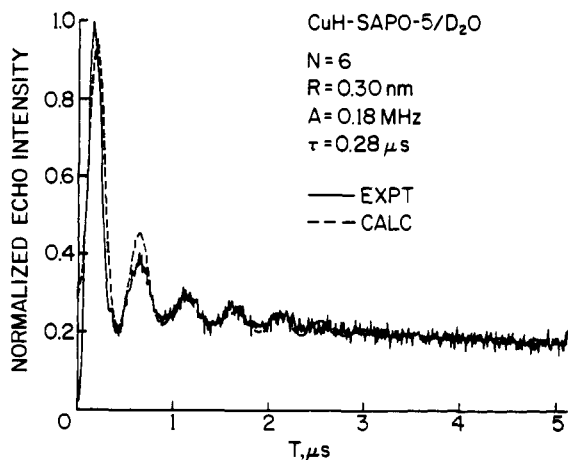


Figure 5. Three-pulse electron spin echo spectra at 4.2 K of CuH-SAPO-5 with adsorbed D_2O .

axially symmetric environment. Rehydration of the activated sample produced an ESR spectrum identical with that of the fresh sample, indicating reversibility of the hydration/dehydration process. Deviations of the g values and hyperfine coupling between the fresh and the activated samples, $g_{\parallel} = 2.394$, $g_{\perp} = 2.074$, $A_{\parallel} = 165 \times 10^{-4} \text{ cm}^{-1}$ for the former and $g_{\parallel} = 2.344$, $g_{\perp} = 2.060$, $A_{\parallel} = 182 \times 10^{-4} \text{ cm}^{-1}$ for the latter, suggest that water significantly varies the local environment of the Cu^{2+} ions. Comparison of these ESR parameters of the fresh sample with those of hydrated CuK-A zeolite¹⁹ indicates octahedral geometry for the Cu^{2+} ions.

Adsorption of $^{15}\text{NH}_3$ on the activated sample gave the ESR spectrum shown in Figure 3. Direct Cu^{2+} -N coordination is indicated by ^{15}N splittings. The hyperfine splitting pattern of ^{15}N

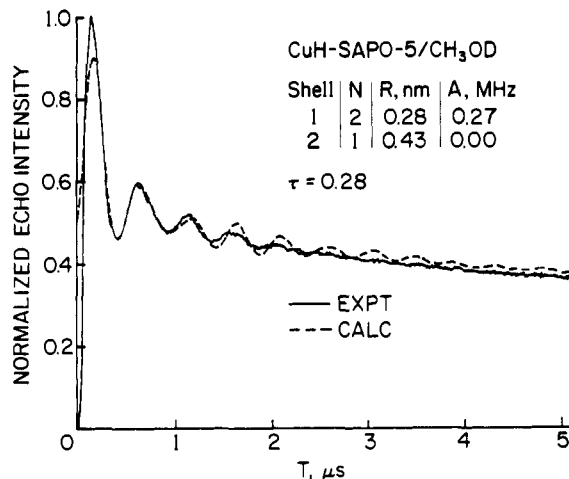


Figure 6. Three-pulse electron spin echo spectra at 4.2 K of CuH-SAPO-5 with adsorbed CH_3OD .

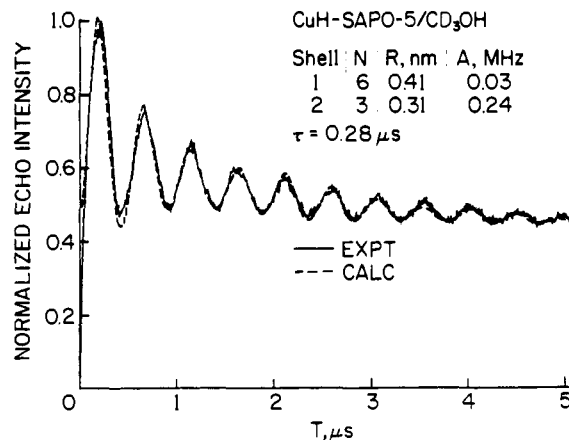


Figure 7. Three-pulse electron spin echo spectra at 4.2 K of CuH-SAPO-5 with adsorbed CD_3OH .

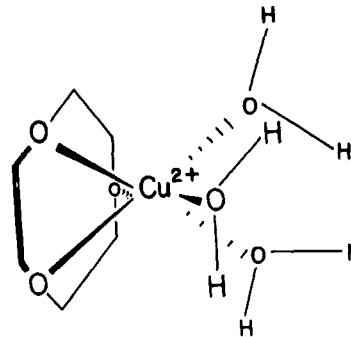


Figure 8. Schematic diagram of a Cu^{2+} ion, located at site II* in an octahedral environment in SAPO-5, directly coordinating to three framework oxygens and three water molecules.

nuclei with nuclear spin $1/2$ shows an intensity ratio of 1:3:3:1, which has been determined by measuring the peak heights from the first-derivative spectrum. This pattern suggests that three equivalent ^{15}N nuclei from three $^{15}\text{NH}_3$ are directly coordinated to a Cu^{2+} ion.

Methanol-adsorbed samples gave somewhat different ESR spectra (Figure 4). The spectra differ from those for an axially symmetric environment in that both spectra have a high-field minimum, which is assigned as g_y here. The reason the high-field minimum is assigned as g_y , rather than as a hyperfine coupling component of g_x is as follows. (1) The hyperfine coupling component of g_x does not extend to such a high field, as evidenced by previous studies of Cu^{2+} ions in an axially symmetric environment.¹² (2) If the high-field component were really a hyperfine coupling line of g_x , other hyperfine lines of g_x would appear at

(19) Narayana, M.; Kevan, L. *J. Chem. Soc. Faraday Trans. 1*, 1986, 82, 213-232.

Table I. ESR Parameters for CuH-SAPO-5

sample treatment ^a	g_{\parallel}^b	$A_{\parallel}^c/10^{-4} \text{ cm}^{-1}$	g_{\perp}^b
fresh	2.394	165	2.074
evac 400 °C	2.344	186	2.060
satd ¹⁵ NH ₃	2.245	204	2.041
satd CH ₃ OD	2.410	145	2.074 ^d 2.050 ^e

^aSatd = saturated with. ^bEstimated uncertainty is ± 0.005 . ^cEstimated uncertainty is $\pm 5 \times 10^{-4} \text{ cm}^{-1}$. ^d g_x value. ^e g_y value.

Table II. Results of ESEM Simulations

adsorbate	shell	N^a	R^b	A_{iso}^c	no. adsorbate molecules
D ₂ O	1	6	0.30	0.18	3
CH ₃ OD	1	2	0.28	0.27	2
	2	1	0.43	0.00	1
CD ₃ OH	1	6	0.41	0.03	2
	2	3	0.31	0.24	1

^aNumber of ²D nuclei. ^bDistance from the Cu²⁺ ion to ²D nuclei, nm. Estimated uncertainty is ± 0.01 nm. ^cIsotropic hyperfine coupling, MHz. Estimated uncertainty is $\pm 10\%$.

the low-field side of g_x . These are absent from both the first-derivative and the second-derivative spectral presentations. Analysis of the spectra gave the following g values: $g_z = 2.410$, $g_x = 2.074$, $g_y = 2.050$. Similar values were reported in a study of Cu²⁺-impregnated silica gel.²⁰ Comparing the ESR parameters of the methanol-adsorbed samples with those of the activated sample suggests that the Cu²⁺ ions directly coordinate with methanol molecules.

Three-pulse ESEM signals (Figures 5–7) recorded from samples adsorbed with D₂O, CH₃OD, and CD₃OH all show ²D modulations, which were simulated without considering the weak quadrupole moment of ²D nuclei. The simulation parameters are listed in Table II. It was quite straightforward to fit the ESEM of the D₂O-adsorbed sample, yielding six ²D nuclei at 0.30 nm. The distance between Cu²⁺ and ²D confirms the direct coordination of D₂O with the Cu²⁺ ion. However, fitting the ESEM signals of methanol-adsorbed samples was not as straightforward, and a two-shell model was used in this case. The ESEM simulation for the CH₃OD-adsorbed sample shows that two ²D nuclei situate at 0.28 nm from the Cu²⁺ ion, indicative of direct coordination of Cu²⁺-OD, and one ²D nucleus situates at 0.43 nm away, indicative of indirect coordination. Simulation of the ESEM signal from CD₃OH yielded six ²D nuclei at 0.41 nm and three ²D nuclei at 0.31 nm. The agreement of the simulation parameters between the samples adsorbed with CH₃OD and CD₃OH will be discussed below.

Discussion

Possible Cation Sites in SAPO-5. In the as-synthesized SAPO-5 molecular sieve, the structure-directing template fills the channels. When the template molecules are removed by calcination, the charge-balancing H⁺ ions in H-SAPO-5 locate at cation sites, as do Cu²⁺ ions in CuH-SAPO-5. By analogy with the designation of cation sites in zeolite X,¹¹ we propose possible cation sites for SAPO-5 (Figure 1). Site I is the center of the double 6-rings that constitute a 6-ring channel. Site II is the center of a 6-ring window that constitutes the side of the 12-ring channel. Site II* is displaced from site II toward the 12-ring channel. The proposed sites II and II* have a local environment rather similar to their counterparts in zeolite X, but proposed site I is less similar to that in zeolite X, because the double 6-rings are connected by three oxygen bridges in SAPO-5 and by six oxygen bridges in zeolite X.

Cu²⁺ Location and Adsorbate Interactions. The probable Cu²⁺ location can be determined on the basis of the ESR and ESEM observations for the Cu²⁺ species in connection with the char-

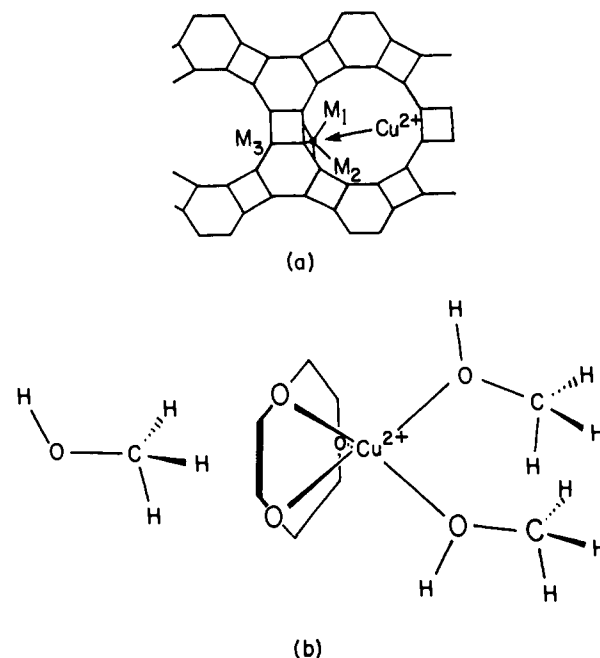


Figure 9. Schematic diagram of a Cu²⁺ ion at site II* in SAPO-5 directly coordinating to two methanol molecules in the same 12-ring channel and indirectly coordinating to one methanol molecule in an adjacent 12-ring channel: (a) relative locations of the Cu²⁺ ion and methanol (M₁, M₂, and M₃) molecules with respect to the SAPO-5 framework; (b) detailed view of the coordination.

acteristics of the SAPO-5 framework structure. ESEM results (Table II) shown that three water molecules situate at a distance of 0.30 nm from a Cu²⁺ ion; ESR results indicate that (1) the waters directly coordinate with the Cu²⁺ ion and (2) the Cu²⁺ ion has an octahedral environment. These facts together suggest that the Cu²⁺ ion is coordinated with three oxygens from the SAPO-5 framework and three oxygens from water molecules. From the SAPO-5 structure, only sites I and site II* permit octahedral geometry so site II can be ruled out. Of site I and II*, the former is not reasonable because Cu²⁺ ion would directly coordinate with six framework oxygens at that site. Site II* is the only possibility left, and a Cu²⁺ ion at this site is able to coordinate directly with three framework oxygens and three water molecules, thus site II* is a reasonable Cu²⁺ location. A similar Cu²⁺ location and adsorbate interaction were reported in Cu²⁺-doped zeolite X.^{7,11}

The Cu²⁺ location in the ammonia-adsorbed sample can also be deduced on the basis of the above discussion. Since three ammonia molecules coordinate directly with one Cu²⁺ ion, resulting in an axially symmetric coordination, site II* is again the only reasonable location for the Cu²⁺ ion. In this case a Cu²⁺ ion coordinates with three framework oxygens and three nitrogens from three ammonia molecules.

The ESEM pattern of the CH₃OD-adsorbed sample reveals that two deuteriums locate 0.28 nm away from a Cu²⁺ ion and one deuterium locates as far as 0.43 nm away. The interaction distances suggest that two methanol molecules are directly coordinated with the Cu²⁺ ion using the hydroxyl oxygens and that another methanol molecule is not directly coordinated. On the other hand, simulation of the ESEM pattern of CD₃OH indicates that six deuteriums locate 0.41 nm away from a Cu²⁺ ion and three deuteriums locate as close as 0.31 nm from the Cu²⁺ ion. Six deuteriums at 0.41 nm in CD₃OH also suggests that two hydroxyl oxygens are directly coordinated with a Cu²⁺ ion. The indirectly coordinated methanol must be oriented in such a way that its methyl group is directed toward the Cu²⁺ ion in order to give a Cu²⁺-D distance of 0.43 nm for CH₃OD and 0.31 nm for CD₃OH. This methanol molecule is likely hydrogen-bonded to the framework in an adjacent 12-ring channel. Apparently, site II* is the only possible Cu²⁺ location, because (1) site I does not permit direct methanol coordination; (2) site II would form a trigonal bipyramidal structure, giving rise to reversed g values ($g_{\parallel} < g_{\perp}$);

(20) Narayana, M.; Zhan, R. Y.; Kevan, L. *J. Phys. Chem.* **1984**, *88*, 3990–3993.

(21) Anderson, M. W.; Kevan, L. *J. Phys. Chem.* **1986**, *90*, 6452–6459.

and (3) when two methanol molecules are coordinated to a Cu^{2+} ion on the same side of a 6-ring window, the Cu^{2+} ion will be pulled away from the window to site II*, even if it were previously inside the window. A similar geometry of Cu^{2+} -methanol coordination has been reported in Cu^{2+} -doped zeolite rho.²¹ The bulky size of the methanol molecule could be a determining factor to account for the fewer adsorbate molecules directly coordinated to the Cu^{2+} ion. From the symmetry, the Cu^{2+} ion at site II* with three framework oxygens and two methanol molecules directly coordinated would not exhibit axial symmetry. This is clearly evidenced by the ESR spectra (Figure 4).

Conclusions

ESR and ESEM results have revealed that, in hydrated CuH-SAPO-5, Cu^{2+} is located at site II*, a cation site inside a 12-ring channel but close to the center of a 6-ring window, directly coordinated to three water molecules in an octahedral geometry. Both the Cu^{2+} location and the ammonia interaction in the am-

monia-adsorbed sample are similar to those in the hydrated CuH-SAPO-5. A nonaxially symmetric Cu^{2+} ESR signal is found for the methanol-adsorbed samples and the ESEM results show that two methanol molecules are directly coordinated with a Cu^{2+} ion and another methanol molecule directs its methyl group toward the Cu^{2+} ion. It is proposed that the Cu^{2+} ion at site II* directly coordinates with the two methanol molecules in the same 12-ring channel and indirectly coordinates with one methanol molecule in an adjacent 12-ring channel. This determination of the Cu^{2+} location and adsorbate interactions is potentially useful for understanding and controlling Cu^{2+} -catalyzed reactions in H-SAPO-5 molecular sieve.

Acknowledgment. We thank Prof. M. Davis for helpful suggestions about the SAPO-5 synthesis, Dr. D. Goldfarb for critical comments, and the U.S. National Science Foundation, the Robert A. Welch Foundation, and the Texas Advanced Research Program for financial support.

Atomic Size Dependence of Bader Electron Populations: Significance for Questions of Resonance Stabilization

Charles L. Perrin

Contribution from the Department of Chemistry, D-006, University of California—San Diego, La Jolla, California 92093-0506. Received October 16, 1989.
Revised Manuscript Received January 2, 1990

Abstract: Model calculations show that the location of the zero-flux surface depends on the size of atomic orbitals that make up the electronic distribution of molecules. As a result, Bader electron populations exaggerate electron densities at electronegative atoms. The resulting atomic charges are judged to be unreliable, especially as evidence against resonance in carboxylate anions and related species.

Introduction

Recently questions have been raised about the importance of resonance stabilization in accounting for the structures of amides and conjugated alkenes and for the acidity of carboxylic acids, carbonyl compounds, and alkenes.^{1,2} The analysis is based in part on atomic charges calculated according to Bader's method for partitioning molecules into atoms.³ This has raised objections, both experimental⁴ and theoretical,^{5,6} as well as a defense,⁷ and experimental data claimed to support the analysis.⁸ However, none of the objections focussed on the fundamental error of the analysis. It is the purpose of this paper to show that these atomic charges have a fatal flaw, since they depend strongly on atomic size.

To assign atomic charges by Bader's method, molecules are partitioned into atomic regions separated by zero-flux surfaces. Such a surface is defined by eq 1, where ρ is the total electron

$$\vec{\nabla}\rho \cdot \vec{n} = 0 \quad (1)$$

density and \vec{n} is the normal to the surface. It can be traced by finding the "critical point" along a bond, where the gradient of electron density is zero (eq 2), and then following paths of steepest

$$\vec{\nabla}\rho = \vec{0} \quad (2)$$

descent from that point. The integrated electron density within a surface is then assigned to the atom within that surface. Therefore, the electron population assigned to an atom depends crucially on the location of the zero-flux surface.

Model Calculations

The influence of atomic size on the location of the zero-flux surface is most clearly seen by considering two *ns* atomic orbitals (AOs), ϕ_A and ϕ_B , of different effective nuclear charge Z_{eff} (Figure 1). Since both these AOs contain a factor $\exp(-Z_{\text{eff}}r/n)$, which falls off rapidly with increasing r , Z_{eff} measures not only electronegativity but also atomic size. In particular, AOs of greater Z_{eff} are smaller. It is easily shown that AO size affects the location of the critical point, independently of electronegativity.

To eliminate the influence of electronegativity so as to focus only on the size effect, we consider the hypothetical case of one electron in each AO, and without any bond between them. Then the electron density ρ is $\phi_A^2 + \phi_B^2$. Along the line A-B, eq 2 becomes eq 3. Moreover, because of the factor $\exp(-Z_{\text{eff}}r/n)$

$$\phi_A \frac{\partial \phi_A}{\partial r} = \phi_A \frac{\partial \phi_A}{\partial x} = \phi_B \frac{\partial \phi_B}{\partial(-x)} = \phi_B \frac{\partial \phi_B}{\partial r} \quad (3)$$

in ϕ , the values of $\phi(\partial\phi/\partial r)$ in eq 3 depend strongly on Z_{eff} and thus on atomic size. At large separations or large r , the value is larger for the AO of smaller Z_{eff} , since this is the more diffuse

(1) (a) Wiberg, K. B.; Laidig, K. E. *J. Am. Chem. Soc.* **1987**, *109*, 5935. (b) Wiberg, K. B.; Laidig, K. E. *Ibid.* **1988**, *110*, 1872. (c) Wiberg, K. B.; Schreiber, S. L. *J. Org. Chem.* **1988**, *53*, 783. (d) Wiberg, K. B.; Breneman, C. M.; LePage, T. J. *J. Am. Chem. Soc.* **1990**, *112*, 61. (e) Wiberg, K. B. *J. Am. Chem. Soc.* **1990**, *112*, 3379, 4177.

(2) Siggel, M. R. F.; Streitwieser, A., Jr.; Thomas, T. D. *J. Am. Chem. Soc.* **1988**, *110*, 8022.

(3) Bader, R. F. W. *Acc. Chem. Res.* **1975**, *8*, 34; **1985**, *18*, 9.

(4) Exner, O. *J. Org. Chem.* **1988**, *53*, 1810.

(5) Dewar, M. J. S.; Krull, K. L. *J. Chem. Soc., Chem. Commun.* **1990**, 333.

(6) Jug, K.; Fasold, E.; Gopinathan, M. S. *J. Comput. Chem.* **1989**, *10*, 965.

(7) Siggel, M. R.; Thomas, T. D. *J. Am. Chem. Soc.* **1986**, *108*, 4360. Thomas, T. D.; Carroll, T. X.; Siggel, M. R. F. *J. Org. Chem.* **1988**, *53*, 1812.

(8) Bennet, A. J.; Wang, Q.-P.; Slebocka-Tilk, H.; Somayajil, V.; Brown, R. S.; Santarsiero, B. D. *J. Am. Chem. Soc.* **1990**, *112*, 6383.